Magnetic Resonance Imaging 79 (2021) 66–75

Contents lists available at ScienceDirect

Magnetic Resonance Imaging

journal homepage: www.elsevier.com/locate/mri

Review article

Myocardial T1-mapping and extracellular volume in pulmonary arterial hypertension: A systematic review and meta-analysis

Samer Alabed [a,b,*], Laura Saunders [a], Pankaj Garg [a], Yousef Shahin [a,b], Faisal Alandejani [a], Andreas Rolf [c], Valentina O. Puntmann [d], Eike Nagel [d], Jim M. Wild [a,e], David G. Kiely [a,f], Andrew J. Swift [a,b,f]

[a] Department of Infection, Immunity and Cardiovascular Disease, University of Sheffield, Sheffield, UK
[b] Department of Clinical Radiology, Sheffield Teaching Hospitals, Sheffield, UK
[c] Department of Cardiology, Kerckhoff-Heart Center, Bad Nauheim, Germany
[d] Institute for Experimental and Translational Cardiovascular Imaging, University Hospital Frankfurt, Frankfurt am Main, Germany
[e] INSIGNEO, Institute for in silico medicine, University of Sheffield, UK
[f] Sheffield Pulmonary Vascular Disease Unit, Royal Hallamshire Hospital, Sheffield, UK

ARTICLE INFO

Keywords:
Myocardial T_1 mapping
Extracellular volume
Pulmonary hypertension
Cardiac MRI
CMR
Meta-analysis

ABSTRACT

Introduction: Elevated myocardial T_1-mapping and extracellular volume (ECV) measured on cardiac MR (CMR) imaging is associated with myocardial abnormalities such as oedema or fibrosis. This meta-analysis aims to provide a summary of T_1-mapping and ECV values in pulmonary arterial hypertension (PAH) and compare their values with controls.

Methods: We searched CENTRAL, MEDLINE, Embase, and Web of Science in August 2020. We included CMR studies reporting T_1-mapping or ECV values in adults with any type of PAH. We calculated the mean difference of T_1-values and ECV between PAH and controls.

Results: We included 12 studies with 674 participants. T_1-values were significantly higher in PAH with the highest mean difference (MD) recorded at the RV insertion points (RVIP) (108 milliseconds (ms), 95% confidence intervals (CI) 89 to 128), followed by the RV free wall (MD 91 ms, 95% CI 56 to 126). The pooled mean T_1-value in PAH at the RVIP was 1084, 95% CI (1071 to 1097) measured using 1.5 Tesla Siemens systems. ECV was also higher in PAH with an MD of 7.5%, 95% CI (5.9 to 9.1) at the RV free wall.

Conclusion: T_1 mapping values in PAH patients are on average 9% higher than healthy controls when assessed under the same conditions including the same MRI system, magnetic field strength or sequence used for acquisition. The highest T_1 and ECV values are at the RVIP. T_1 mapping and ECV values in PH are higher than the values reported in cardiomyopathies and were associated with poor RV function and RV dilatation.

1. Introduction

Native myocardial T1 and extracellular volume (ECV) mapping have shown promise as novel biomarkers to support diagnostic, therapeutic and prognostic decision making in several cardiovascular disorders [1]. T_1 mapping produces a pixel-by-pixel representation of the longitudinal relaxation times (T1) within a tissue [2]. This relaxation time can be measured on a MRI system and sequence-specific standardised scale to provide surrogate tissue characterisation data [3]. In the myocardium, T_1 times are affected by two main factors; oedema and collagen in the interstitial space [4]. Oedema can be secondary to inflammation or infarction, whereas increased collagen is associated with fibrosis or

Abbreviations: ANGIE, Accelerated and Navigator-Gated Look-Locker Imaging; CI, confidence interval; CMR, cardiac magnetic resonance; CTEPH, chronic thromboembolic pulmonary hypertension; ECV, extracellular volume; HFpEF, heart failure with preserved ejection fraction; LV, left ventricle; MOLLI, MOdified Look-Locker Inversion Recovery; mPAP, mean pulmonary artery pressure; MD, mean difference; MRI, magnetic resonance imaging; ms, millisecond; PAH, pulmonary arterial hypertension; PH, pulmonary hypertension; RV, right ventricle; RVEF, right ventricle ejection fraction; RVIP, right ventricle insertion point; SASHA, Saturation Recovery Single-Shot Acquisition; SD, standard deviation; T, tesla.

* Corresponding author at: Cardiac MRI Research Fellow and Specialist Registrar in Cardiac Radiology, Department of Infection, Immunity and Cardiovascular Disease, University of Sheffield, Glossop Road, Sheffield S10 2JF, United Kingdom.
E-mail address: s.alabed@nhs.net (S. Alabed).

https://doi.org/10.1016/j.mri.2021.03.011
Received 17 November 2020; Received in revised form 10 March 2021; Accepted 13 March 2021
Available online 18 March 2021

infiltrative processes [5–8]. An elevated T_1 value is, therefore, a non-specific tissue composition marker for conditions such as myocardial infarction, myocarditis, cardiomyopathies and diastolic heart failure [6,9–16]. A low T_1 is being used as a diagnostic tool and follow-up biomarker in Anderson-Fabry disease [17–21] and can be used as a complementary sequence to T2* in thalassemia [22,23].

Performing T_1 mapping after contrast administration enables the assessment of the extracellular space [1,4]. As gadolinium collects in the extracellular fluid, its paramagnetic effect causes shortening of the T_1 values of the myocardium. The T_1 shortening is proportional to the concentration of the gadolinium in the extracellular fluid. Therefore, combining pre- and post-contrast T_1 values of the myocardium and blood pool with the haematocrit allows estimation of the extracellular volume (ECV) [1]. Elevated ECV is seen with myocardial fibrosis or oedema and is associated with an increased risk for mortality [24–26]. Native T_1 and ECV can provide prognostic information in coronary artery disease and nonischemic cardiomyopathies [4,27,28] and might play a role in disease risk stratification, early diagnosis and monitoring progression [2,13,14].

In pulmonary arterial hypertension (PAH), elevated pulmonary artery pressure causes significant afterload on the right ventricle (RV). Eventually, the RV hypertrophies and dilates triggering a fibrogenic process [29]. T_1 mapping and ECV might, therefore, play a role in evaluating the changes in the RV [30] and the degree of fibrosis in PAH [29].

Previous reviews have assessed normal T_1 mapping and ECV values in healthy people [31] and pathological values in cardiomyopathies [32–34]. Several studies report T1 values in PAH, but there is currently no meta-analysis to summarise their results. This meta-analysis aims to compare the range of T_1 values and ECV in PAH to control participants and identify the regions of the myocardium with the highest T_1 values.

2. Methods

The review was prospectively registered with The International Prospective Register of Systematic Reviews on 10/02/2020 (ID: CRD42020166392).

2.1. Criteria for considering studies for this review

We considered any study comparing T_1 mapping or ECV values in adult patients with PAH and controls; such as controlled trials, cohort studies or case-control studies. Studies with less than 10 participants and case reports were excluded. Inclusion was considered irrespective of prospective or retrospective recruitment, publication date, publication status or language.

2.2. Outcomes

1. The pooled mean difference of T_1 value and ECV between PAH and controls
2. Identifying the myocardial region with the largest T_1 values and ECV in PAH
3. Comparing the T_1 values in the subgroups of PAH

2.3. Search methods for identification of studies

The following databases were systematically searched for relevant studies on 08/08/2020: i) Cochrane Central Register of Controlled Trials (CENTRAL) ii) MEDLINE (ProQuest, 1946 to Aug 2020) iii) Embase (Ovid, 1974 to 2020 Week 32) and Web of Science. The search strategy used is outlined in the Appendix.

The reference lists of all relevant articles identified during the full-text screening were scrutinised for relevant studies.

2.4. Statistical analysis and data synthesis

We used Review Manager 5.4 (The Cochrane Collaboration, 2020) to perform a meta-analysis of the mean differences (MD) and produce the forest-plot. A random-effect model with 95% confidence intervals (CI) was used in the analyses. The available data allowed us to calculate the mean difference for 1.5 T field strength only.

We pooled the means and standard deviations (SD) of T_1 values for the PAH and control groups when they were measured using the same MRI system and field strength, which was only possible for 1.5 T Siemens systems. The non-weighted means of T_1 values with their 95% CI for PAH patients and controls were presented on a forest plot using GraphPad Prism version 8.3 (GraphPad Software, La Jolla CA, USA). If the T1 and ECV values for the RV insertion points were measured both at the superior and inferior insertion points, data for the inferior insertion points were chosen, as this was the case with the majority of the studies. A funnel plot to assess publication bias was not performed as the number of included studies in each meta-analysis were too low to identify real asymmetry [35].

3. Results

3.1. Results of the search

Our comprehensive search identified a total of 12 studies that were included in the meta-analysis. Nine studies reported T_1 mapping values in PAH [36–44] including one conference abstract [45] and five studies reported ECV values [37–39,46,47]. The details of the literature search are presented in the PRISMA flow diagram (Fig. 1).

3.2. Description of included studies

3.2.1. Study design

The review includes nine case-control studies and three case-series published between 2015 and 2020. Prospective recruitment was performed in seven studies and retrospective recruitment in five studies. Only three studies had a sample size $\geq$60. The largest study was Saunders 2018 with 223 PAH patients and 24 controls.

3.2.2. Population

The studies were conducted in 8 different countries; 6 studies were conducted in Europe, 2 in the USA and 4 in Japan and China. The studies included 554 PH patients of which 513 (93%) had PAH, 32 (6%) had chronic thromboembolic pulmonary hypertension (CTEPH) and 9 (1%) had PH secondary to lung disease. The control group included 120 people, of whom 97 were healthy and 23 were non-PH patients. The age of patients with PAH was 53 $\pm$ 15 years and 64% were women with a pooled average mPAP of 48 $\pm$ 15 mmHg, and RVEF of 42 $\pm$ 14%. The control group had a pooled average age of 49 $\pm$ 7 years and 52% were women. The pooled average of RVEF was 55 $\pm$ 5%. Details of included studies are presented in Table 1.

3.2.3. MRI systems and T_1 techniques

The majority of studies were performed using 1.5 Tesla field-strength MRI systems. A 3 Tesla system was used in Asano 2018, Dong 2018 and Reiter 2017 [40,45,47]. Siemens MRI scanners were used in most studies apart from Saunders 2018 and Homsi 2017 who used a GE and Philips MRI system, respectively [37,41]. A modified look-locker inversion recovery (MOLLI) sequence was used in all studies apart from Mehta 2015 who used accelerated and navigator-gated look-locker imaging for cardiac T_1 estimation (ANGIE) [38]. T_1 mapping values were measured on short-axis images on a single mid-chamber slice [41,42,44,46,47], single basal slice [43], average of two mid-chamber slices [38], average of a basal and a mid-chamber slice [36,39] or averaged over basal, mid-chamber and apical slices [37,40]. T_1 values were measured in end-diastole, apart from Mehta 2015 and Reiter 2017 who measured T_1

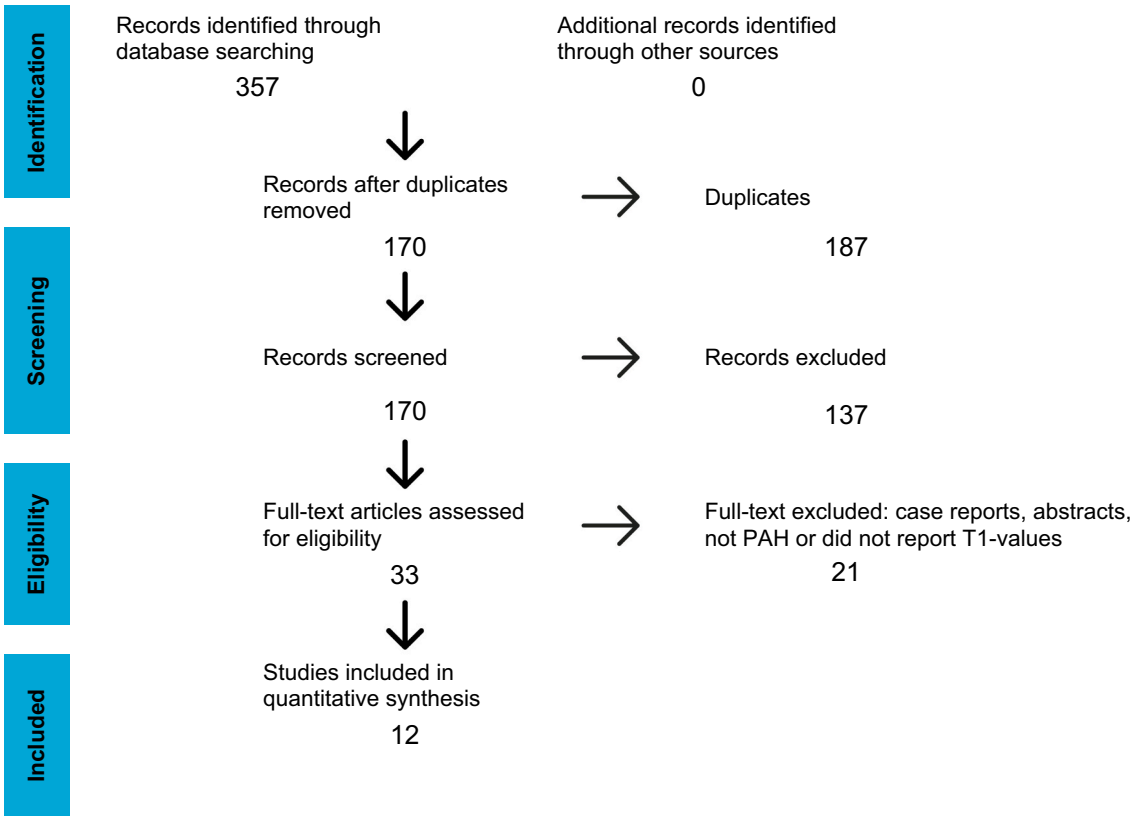

Fig. 1. PRISMA Flow Chart.

values in systole [38,40]. None of the included studies used stress MRI to assess T_1 values. Details of the MRI systems, techniques and sequences used are provided in Table 2.

3.3. Results of the Meta-analysis of the T_1 values and ECV

3.3.1. The mean difference of T_1 value in PAH and controls

Seven studies compared myocardial T_1 values at 1.5 Tesla between 375 PAH patients and 87 healthy controls. The T_1 values in PAH are significantly larger than the T_1 values of the control group. The largest difference was reported at the RVIP (MD 108 ms, 95% CI 89 to 128), followed by the RV free wall (MD 91 ms, 95% CI 56 to 126). The mean difference at the mid septum and LV lateral wall were relatively smaller (MD 56 ms, 95% CI 41 to 72) and (MD 36 ms, 95% CI 14 to 58), respectively. The forest plot of the meta-analysis of mean differences between PAH and controls is presented in Fig. 2.

Two studies reported myocardial T_1 values at 3 Tesla; Reiter 2017 and Asano 2018 [40,45]. However, their results could not be pooled as they reported T_1 values at different regions of the myocardium. In addition, Reiter 2017 included non-PH patients as the control group, whereas Asano 2018 included healthy people. The highest calculated mean difference of the T_1 values in Reiter 2017 was 105 ms, 95% CI (76 to 133) at the RVIP. The mean difference at the septum and LV lateral wall were smaller 63 ms, 95% CI (40 to 86) and 40 ms, 95% CI (20 to 60), respectively. In Asano 2018 the calculated MD at the RV free wall was 178 ms, 95% CI (134 to 222).

3.3.2. T_1 values in different myocardial regions

Comparing the mean difference in the T_1 values in different myocardial regions measured within PAH patients showed that the T_1 values at the RVIP is on average 6% higher than the septum (MD 62 ms, 95% CI 49 to 74) and 9% higher than the LV lateral wall (MD 102 ms, 95% CI 82 to 121). The pooled mean value of T_1 with a 1.5 T Siemens system for PAH patients and healthy controls are shown in Table 3 and their ranges are illustrated in Fig. 4. The T_1 values for PAH were pooled including values reported in the case series Tello 2019 and Habert 2020. Excluding the results of Mehta 2015, who used ANGIE sequences, did not significantly change the pooled values.

3.3.3. T_1 values in different PAH subgroups

Three studies compared T_1 values in 140 patients with idiopathic PAH to T_1 values in 118 patients with PAH associated with CTD or CHD [37,41,42]. These studies showed no significant differences in the T_1 mapping values between the different PAH subgroups (MD 4 ms, 95% CI -18 to 26).

3.3.4. ECV mean difference

Five studies reported ECV values in PAH. Three used a 1.5 T Siemens and one a 1.5 [38,39,46], one a 1.5 T Philips system [37] and one a 3 T Siemens scanner [47]. Three studies compared the value of myocardial ECV at 1.5 T between PAH and healthy controls [37–39]. Due to the limited data pooling the mean differences of ECV values was only possible for the RV free wall and LV lateral wall and was significantly higher in PAH compared to the control group at both sites with a mean difference of 7.5%, 95% CI (5.9 to 9.1) at the RV free wall and 4.8%, 95% CI (1.6 to 8.1) at the LV free wall. The mean difference at the RVIP was reported in Homsi 2017 as 5.8%, 95% CI (2.2 to 9.4) and at the septum as 5.7%, 95% CI (3 to 8.4). The forest plot of the meta-analysis of mean differences is presented in Fig. 3.

3.3.5. ECV values in different myocardial regions

Limited data reporting ECV values was available and only ECV values measured at the RV and LV free walls using a 1.5 T Siemens scanner could be pooled (Table 3 and Fig. 4). Dong 2018 evaluated ECV values with a 3 T Siemens system and reported a value of 29.3% ± 4.9 at the septum and 38.5% ± 3.9 at the RVIP.

Table 1
Study characteristics.

	Study author year	Country	Design	Study period	Group	Size	Sex F %	Age	Heart rate	mPAP	RVEF	PH Type
PAH and control	Asano 2018	Japan	RCC	2015–2017	PH	30	N.R	N.R	N.R	41 ± 13	N.R	100% PAH
					Control	10	N.R	N.R	N.R	N.R	N.R	Healthy
	Chen 2017	China	PCC	2015–2016	PH	22	73%	40 ± 13	74 ± 8	60 ± 18	35 ± 11	PAH 82%, CTEPH 18%
					Control	10	60%	38 ± 14	70 ± 7	N.R	56 ± 6	Healthy
	Homsi 2017	Germany	PCC	2014–2015	PH	17	47%	64 ± 14	74 ± 10	N.R	40 ± 13	PAH 100%
					Control	20	50%	63 ± 11	66 ± 14	N.R	55 ± 3	Healthy
	Mehta 2015	USA	RCC	N.R	PH	12	67%	61 ± 19	N.R	N.R	36 ± 10	PAH 83%, CTEPH 17%
					Control	10	80%	24 ± 3	N.R	N.R	55 ± 5	Healthy
	Patel 2020	USA	PCC	2014–2016	PH	13	77%	59 ± 16	81 ± 16	48 ± 8	44 ± 11	PAH 100%
					Control	8	38%	71 ± 4	64 ± 9	N.R	53 ± 4	Healthy
	Reiter 2017	Austria	PCC	2012–2015	PH	35	57%	64 ± 16	74 ± 12	44 ± 13	41 ± 14	PAH 51%, CTEPH 23%, Lung disease 20%, Other 6%
					Control	23	70%	59 ± 12	68 ± 11	18 ± 4	54 ± 7	Non-PH patients
	Saunders 2018	UK	RCC	2015	PH	223	67%	55 ± 16	72 ± 14	46 ± 15	45 ± 15	PAH 100%
					Control	24	51%	58 ± 4	N.R	N.R	N.R	Healthy
	Spruijt 2016	Holland	RCC	2011–2014	PH	70	73%	54 ± 16	79 ± 14	47 ± 13	42 ± 16	PAH 86%, CTEPH 14%
					Control	10	40%	20 ± 1	74 ± 11	N.R	N.R	Healthy
	Wang 2018	China	PCC	N.R	PH	18	44%	61 ± 12	N.R	44 ± 13	38 ± 11	PAH 100%
					Control	5	60%	37 ± 13	N.R	N.R	55 ± 3	Healthy
PAH only	Dong 2018	China	RCS	2016–2017		60	65%	35 ± 15	81 ± 16	59 ± 20	40 ± 12	PAH 100%
	Habert 2020	France	PCS	2012–2013		12	50%	50 ± 16	N.R	44 ± 12	40 ± 18	PAH 83%, CTEPH 17%
	Tello 2019	Germany	PCS	2016–2018		42	52%	56 ± 13	N.R	43 ± 14	38 ± 13	PAH 86%, CTEPH 14%

ANGIE, Accelerated and navigator-gated look-locker imaging; CTEPH, chronic thromboembolic pulmonary hypertension; MOLLI, Modified Look-Locker inversion recovery; mPAP, mean pulmonary artery pressure; n, number; N.R, not reported; PAH, pulmonary arterial hypertension; PHpH, pulmonary hypertension; PCC, prospective case-control; PCS, prospective case series; RCC, retrospective case-control; RCS, retrospective case series; RVEF, right ventricle ejection fraction; T, tesla.

4. Discussion

In this systematic review and meta-analysis, we demonstrate a significant rise in myocardial T_1 values in patients with PAH when compared to healthy controls scanned under the same conditions, confirming potential diagnostic value in measuring T_1 mapping in PAH. The myocardial region with the largest difference between PAH and healthy controls was the RVIP with a mean difference of 108 ms, 95% (CI 89 to 128). The mean difference at the septum was 63 ms, 95% CI (40 to 86) and at the LV free wall 40 ms, 95% CI (20 to 60). The pooled T_1 value at the RVIP on 1.5 Tesla Siemens system and MOLLI sequence was 1084 ms, 95% CI (1071 to 1097), which is on average 9% higher than in healthy people. Therefore the RVIP should be used to measure T_1 mapping values in suspected PAH. The pooled normal T_1 values at the septum on 1.5 T Siemens scanners in our meta-analysis were 988 ms, 95% CI (978 to 998) which are similar to the values reported in a large meta-analysis of normal T1 values of 977 ms, 95% CI (969 to 985) [31].

Limited data exists on ECV values in PAH. The highest mean difference of ECV in PAH compared to healthy people was at the RV free wall and measured 7.5%, 95% CI (5.9 to 9.1) on 1.5 Tesla Siemens systems.

The T_1 values in PAH and the mean difference in T_1 values between PH and healthy controls is higher than what is reported in cardiomyopathies [33,34]. The mean difference in septal T_1 values were 45 ms, 95% CI (31 to 60) in dilated cardiomyopathies and 47 ms, 95% CI (33 to 62) in hypertrophic cardiomyopathies compared to healthy controls [33]. Reiter 2017 assessed the difference between PH patients and patients with cardiomyopathies which is more realistically seen in a clinical setting [40]. They found that at 3 T there remained a significant difference between the patient groups (105 ms) at the insertion points. Saunders 2018 found the differences smaller on a 1.5 T scanner. The T_1 values at the RVIP were 1065 ± 86 ms in PH patients compared to 1017 ± 69 ms in non-PH patients and 943 ± 52 ms in healthy volunteers [41]. Myocardial T_1 mapping might therefore not be able to differentiate between PAH and other cardiac abnormalities at 1.5 T but it would indicate an underlying pathological process increasing the mechanical strain on the RV. The elevated T_1 values at the insertion point in particular might represent engorgement of extracellular spaces in the early phases [25] or fibrosis in more advanced stages of PAH [48].

We pooled the results of different subtypes of PAH including idiopathic PAH, PAH secondary to connective tissue disease (CTD) and congenital heart disease (CHD). CTD and CHD are known to generate fibrosis in the RV and septum the current studies [49–52] and particularly CTD has shown elevated T_1 values [53]. However, three included studies reporting different subtypes of PAH showed no significant differences with the T_1 mapping values seen in idiopathic PAH compared to PAH secondary to CTD or CHD [37,41,42]. Therefore, pooling the

Table 2
Study T_1 mapping systems, sequences and parameters.

Study author year	MRI system	FS (Tesla)	Technique	Sequence protocol	TE/TR (ms)	Flip angle	Spatial resolution mm2	Slice thickness (mm)	Slices measured	FOV (mm)	Partial Fourier Technique	Parallel imaging factor	Software used
Asano 2018	Siemens, Magnetom Verio	3	MOLLI	N.R	N.R	N.R	N.R	N.R	N.R	N.R	N.R	N.R	N.R
Chen 2017	Siemens, Magnetom Aera	1.5	MOLLI	5(3)3	1.1 / 2.3	35	1.4 × 1.4	8	Mean of basal and mid-chamber	360 × 360	7/8 reconstruction	GRAPPA 2	Argus, Siemens
Homsi 2017	Philips, Ingenia	1.5	MOLLI	3(3)3 (3)5	1 / 2.2	35	1.2 × 1.2	10	Mean of basal, mid-chamber and apex	300 × 300	N.R	SENSE 2	Segment, Medviso
Mehta 2015	Siemens, Magnetom Avanto	1.5	ANGIE	5 (4)3	1.6 / 3.2	35	1.2–1.4 × 1.2–1.4	4	Mean of two mid-chamber slices (end-systole)	270 × 340	no	factor 2	Argus, Siemens
Patel 2020	Siemens, Magnetom Aera	1.5	MOLLI	5(3)3	N.R	35	1 × 1	8	Mean of basal and mid-chamber	280 × 210	6/8 reconstruction	GRAPPA 2	MASS, Medis
Reiter 2017	Siemens, Magnetom Trio	3	MOLLI	5(4)2	1.1 / 2.6	35	2.1 × 1.4	8	Mean of basal, mid-chamber and apex (in systole)	315 × 360	6/8 reconstruction	GRAPPA 2	Argus, Siemens
Saunders 2018	GE, HDx	1.5	MOLLI	3(3)5	1.41 / 3.2	35		5.1	Single mid-chamber	400	N.R	2	GE Advantage Workstation
Spruijt 2016	Siemens, Magnetom Avanto	1.5	MOLLI	3(3)5	N.R	N.R	N.R	N.R	Single mid-chamber	N.R	N.R	N.R	N.R
Wang 2018	Siemens, Magnetom Avanto	1.5	MOLLI	N.R	1.17 / 2.4	35	1.71 × 1.67	8	Single mid-chamber	240 × 330	N.R	N.R	MASS, Medis
Dong 2018	Siemens, Magnetom Trim Trio	3	MOLLI	5(3)3	1.12 / 2.9	35	2.4 × 1.8	8	Single mid-chamber	320 × 340	N.R	2	MASS, Medis
Habert 2020	Siemens, Magnetom Symphony	1.5	MOLLI	5(3)3	1.2 / 2.4	35	2.3 × 2.3	7	Single mid-chamber	N.R	N.R	N.R	Argus, Siemens
Tello 2019	Siemens, Magnetom Avanto	1.5	MOLLI	3(3)5	1.06 / 740	35	2.2 × 1.8	8	Single basal	240 × 340	6/8 reconstruction	N.R	Argus, Siemens

FS, field strength; MOLLI, Modified Look-Locker inversion recovery; MRI, Magnetic resonance imaging; ms, milliseconds; N.R, not reported; TE,echo time; TR, repetition time;
CI, confidence intervals; ECV, extracellular volume; LV, left ventricle; ms, milliseconds; PAH, pulmonary arterial hypertension; N, number; NA, not available; RV, right ventricle; RVIP, Right ventricular insertion points;

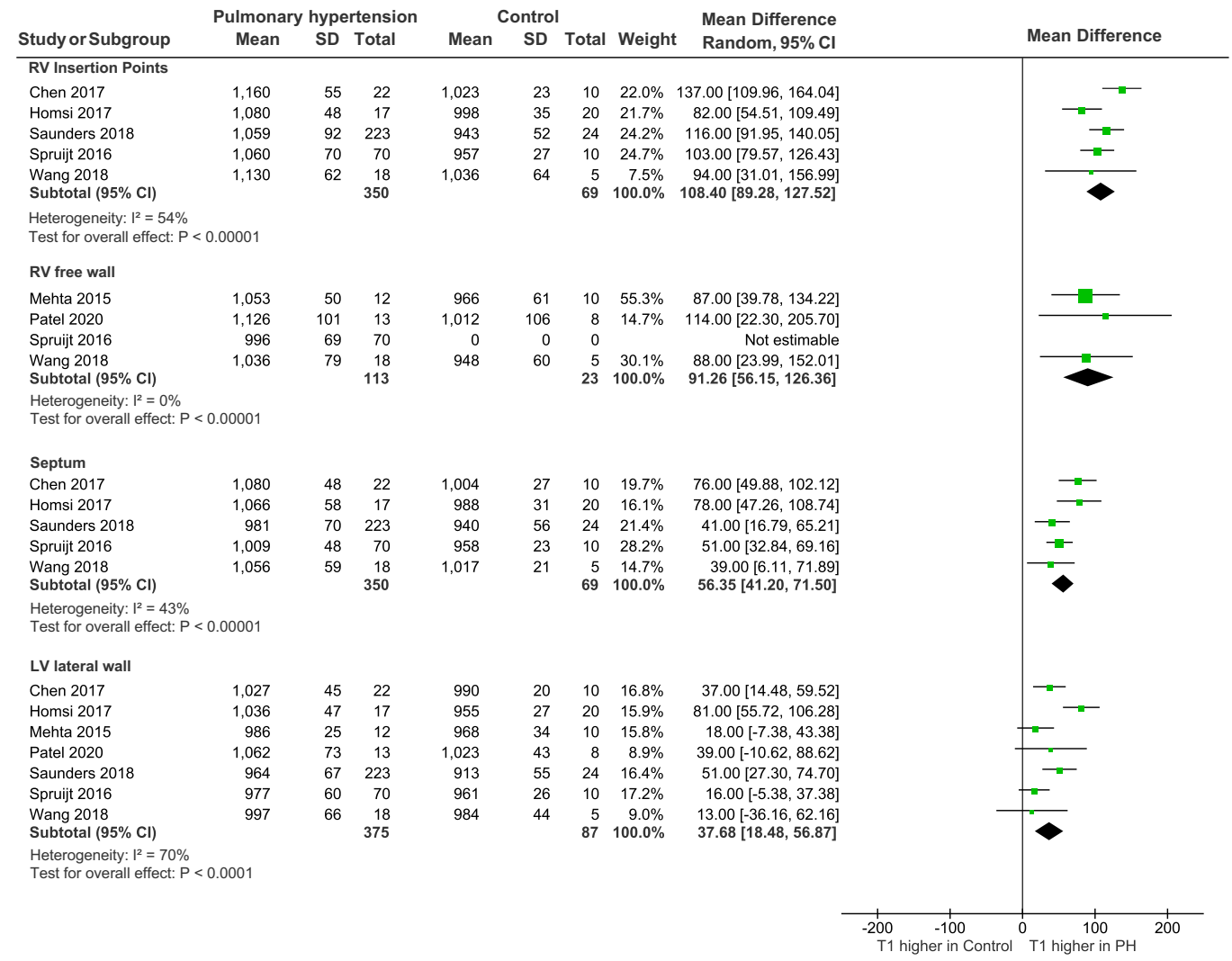

Fig. 2. Forest plot of the mean difference of T_1 values in PAH and controls.
T_1 values in PAH were significantly higher than controls assessed under the same conditions. The mean difference is pooled for myocardial region separately.
CI, confidence intervals; ECV, extracellular volume; ms, millisecond; LV, left ventricle; PH, pulmonary hypertension; RV, right ventricle; SD, standard deviation.

results of the subgroups of PAH was considered appropriate.

T_1 values [36,41] and ECV [38,46] significantly correlated to RV function and volumes. This is in agreement with similar findings in nonischemic cardiomyopathies, which showed an association between elevated T_1 at the RVIP and RV dysfunction [54]. Deterioration in RV function is associated with a poor prognosis in PAH [55,56]. However, Saunders 2018 found that myocardial T_1 mapping did not predict mortality. During a median follow-up of 27 months, they reported 59 deaths from 369 included patients. Their univariate Cox regression showed that RV ejection fraction, end-diastolic and end-systolic RV volumes, RV mass index and the septal angle were prognostic markers, but not T_1 values [41].

Areas with late gadolinium enhancement (LGE) showed a high T_1 value and ECV in Homsi 2017 and were associated with a significantly impaired RV function [37]. LGE at the RVIP is linked to focal fibrosis and more severe disease [48,50,57–60]. T_1 values and ECV remained significantly higher in PAH compared to controls even in the absence of LGE, which may indicate that myocardial T_1 mapping is more sensitive than LGE and could serve as an early marker for fibrosis [37]. This observation is in keeping with findings in patients with PH secondary to CTEPH [61] and findings of a porcine model of chronic PH, where T_1 values and ECV were elevated in areas of fibrosis before the onset of LGE [62].

Almost all included studies used the MOLLI myocardial T_1 mapping sequences, while Mehta 2015 used ANGIE sequences [38]. However, even within MOLLI sequences there are a multitude of sequence parameters. The accuracy and precision of MOLLI sequences are highly dependent on several factors including flip angle, inversion times, recovery times, numbers of inversions, off-resonance, heart rate, spatial resolution, parallel imaging and field strength to mention some [63]. The primary meta-analysis compared PAH patients with controls imaged under the same conditions and therefore any differences in image acquisition does not affect the result of the meta-analysis. However, patients with PAH are more likely to have a higher heart rate than controls. When stroke volume decreases cardiac output is compensated by increased heart rate. The MOLLI sequence is heart rate sensitive owing to the time between inversion and the influence of the readout during each inversion recovery. The effect is that when 'normal heart rate' MOLLI is used in a high heart rate situation the T1-values can be expected to be falsely lower. Many of the studies pooled in the meta-analysis have T_1-values within the higher limit of normal range, even in the insertion point area. These values could be falsely normal if

Table 3
Pooled T_1 and ECV values at different myocardial regions (1.5 T Siemens).

Myocardial region	Group	T1 values [ms] (95% CI)	N Studies (participants)	ECV [%], (95% CI)	N Studies (participants)
RVIP	PAH	1084 (1071 to 1097)	4 (152)	NA	NA
	Healthy controls	999 (985 to 1014)	3 (25)	NA	NA
Septum	PAH	1021 (1012 to 1030)	4 (152)	34.2 (30 to 44)	1 (12)
	Healthy controls	988 (978 to 998)	3 (25)	NA	NA
RV free wall	PAH	1017 (1006 to 1028)	6 (167)	34 (32.5 to 35.5)	3 (37)
	Healthy controls	978 (944 to 1012)	3 (23)	26.6 (24.9 to 28.3)	2 (18)
LV free wall	PAH	997 (987 to 1007)	5 (135)	30.4 (29 to 31.8)	3 (37)
	Healthy controls	984 (975 to 992)	5 (43)	26 (24.7 to 27.4)	2 (18)

'normal heart rate' MOLLI sequences were used.

Repeatability of T_1-values was high in Saunders 2018 and Chen 2017 and was highest at the septum followed by the RVIP. Intraobserver T_1-values varied by up to 20 ms in Chen 2017. The high agreement between readers, confirms that there is good repeatability of T_1 measurement when the same system, parameters and sequences are used [63,64]. A standardised method of measuring T_1 values might support the myocardial T_1 mapping technique becoming more reliable in the assessment of PH [65]. Deep learning methods for the automated quantification of T_1 mapping and ECV are being developed and have shown good performance compared to manual assessment [66]. However, the repeatability of T_1 mapping between different scanners can vary considerably even when using the same sequences and field strength [67] which can limit its utility as a follow-up tool. MRI Harmonisation techniques have been proposed to reduce inter-scan and inter-site variability by adjusting MRI data to a correction factor [68]. Several methods have been suggested for estimating correction factors such as using data from matched controls or travelling subjects between sites [69]. The correction covariate applied at a voxel level can bring T_1 values from different sequences into a unified space for a more accurate quantitative comparison of percent differences in T1 and ECV values between normal and PAH subjects.

RV free wall T_1 mapping was assessed in five studies [38,39,42,44,45]. T_1 mapping at the RV free was significantly higher compared to the LV lateral wall in the same patient and compared to the RV free wall in healthy control. The increase of T_1 values in a thickened RV free wall compared to the LV free wall may reflect the increased pressure and afterload on the RV in PH [54]. However, despite this, assessing the T_1 value at the RV free wall remains challenging. The partial volume effects from the adjacent blood pool or epicardial fat is truly an issue particularly as image slices are currently thicker than the RV wall itself. Sequences with higher spatial resolution might allow better assessment of the thin RV free wall such as the ANGIE sequences

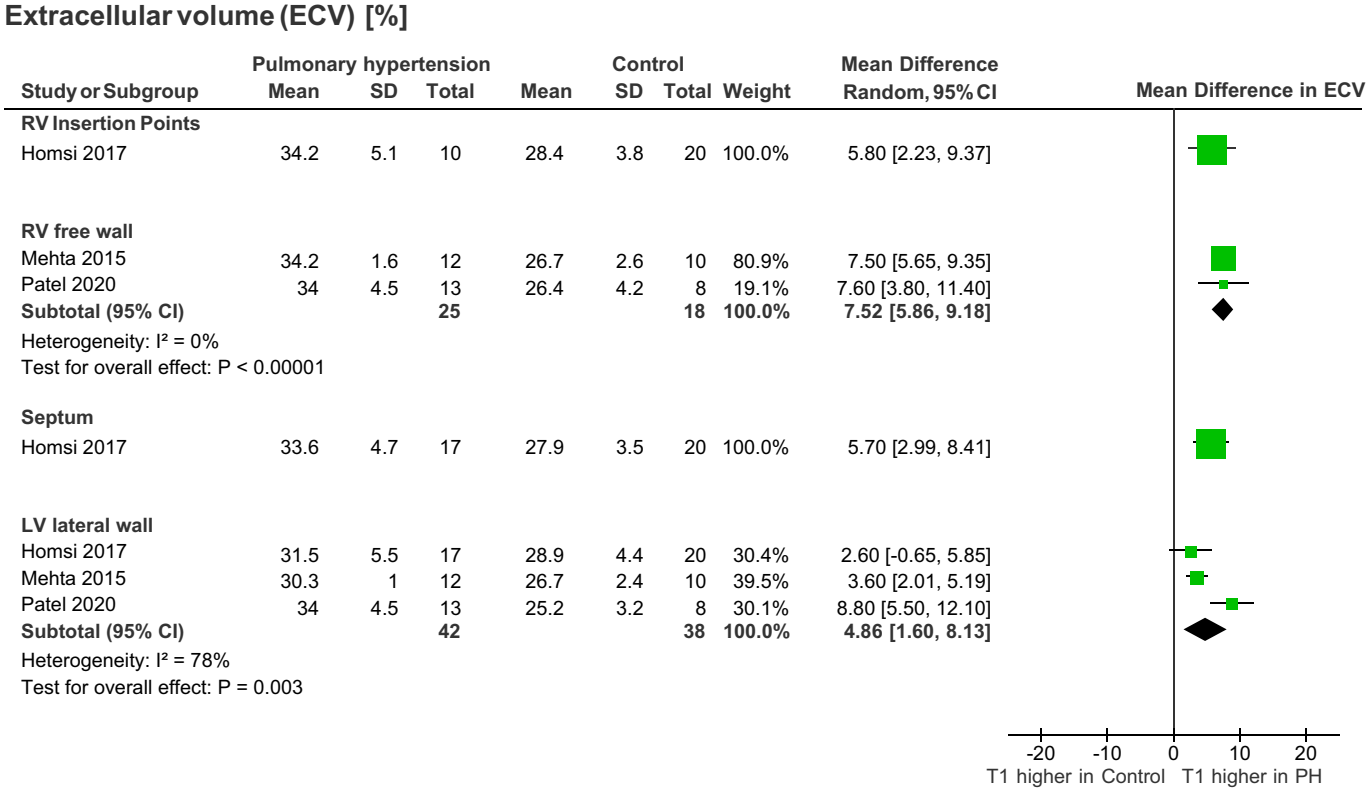

Fig. 3. Forest plot of the mean difference of ECV in PAH and controls.
For abbreviation list see legend for Fig. 2.

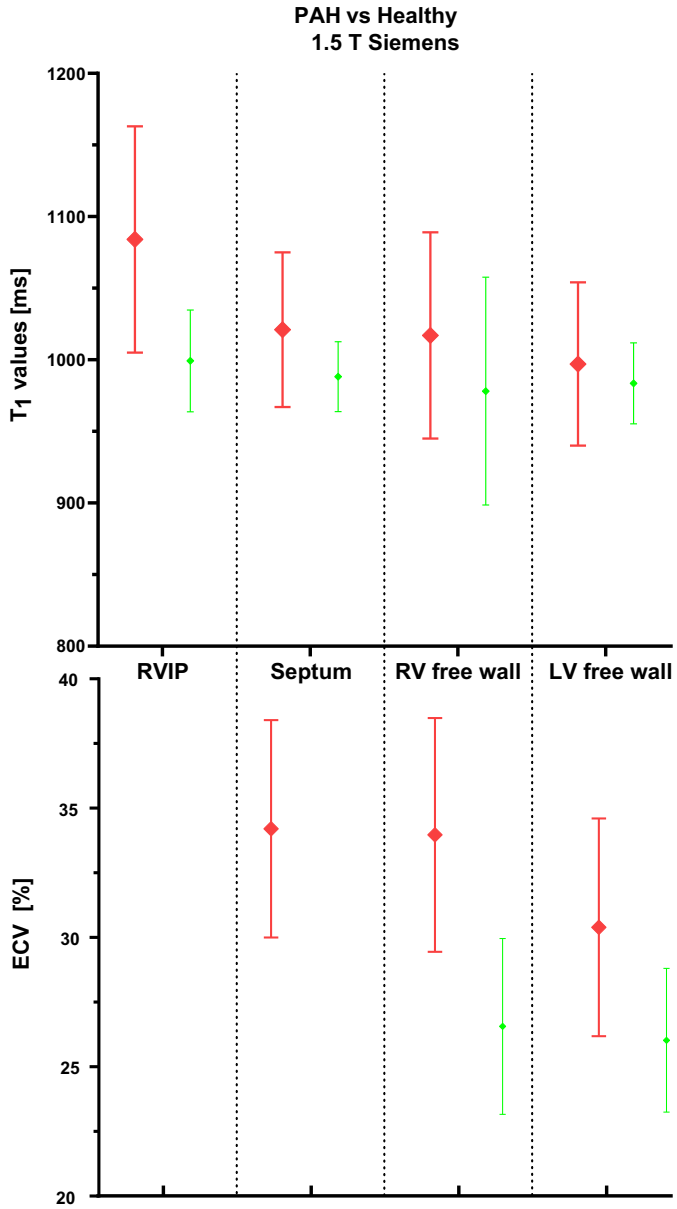

Fig. 4. Pooled T_1 and ECV values in PAH and controls on 1.5 T Siemens.
The T_1 values measured on 1.5 T Siemens systems were pooled together. T_1 values are significantly higher in PAH (red lines) compared to healthy controls (green lines) in all myocardial regions. There is overlap in the T_1 value ranges at the septum and LV and RV free walls, however the overlap was the lowest at the RVIP where the T_1 values most distinguished between PAH and controls. Limited data was available for ECV but again this showed significant differences between PAH and controls.
For abbreviation list see legend for Fig. 2.

used by Mehta 2015 employed [38]. However, technical problems eliciting T_1 values can also be caused by the relative asymmetrical shape of the RV with its curved wall at midventricular level and its myocardial trabeculation [54]. Mehta 2015 tried to overcome this by measuring T_1 values of the RV free wall in end-systole when the RV is at its thickest. While this might facilitate obtaining a T_1 value reading, it is not as accurate or reliable as diastolic T_1 maps and more likely to cause false values. In systole the likelihood of including RV trabeculations and hence blood is increased when the borders of trabeculations/compact myocardium are less distinguishable. Assessing the T_1 value in a thin RV free wall in healthy people is particularly difficult [41,42]. In Spruijt 2016 it was not feasible to draw regions of interest in the RV free wall in the majority of PAH patients and the healthy controls because the RV free wall was too thin and the partial volume effects too substantial, emphasising the concerns and limited benefit of measuring T_1 values at the RV free wall.

4.1. Limitations

The strength of the meta-analysis is the extensive literature search that identified all reported myocardial T_1 mapping and ECV values reported in PAH. The main limitation is that the analysis is based on mainly small retrospective studies. The variation in MRI systems and field strength limited the number of meta-analyses possible. The main analysis pooled the differences between T1 mapping values in PAH and healthy volunteers measured under the same condition to reduce the effect of variations between T_1 mapping estimation methods across studies. However, pooling the actual T_1 mapping values across studies is

prone to heterogeneity from several sources including imaging sites, MRI systems, sequences, techniques and slice selection. ECV was only reported in five studies using different techniques and a mean ECV value could not be calculated. PH is a group of very diverse diseases that vary in the mechanisms of affecting pulmonary artery pressure, resistance and morphology and have different RV remodeling responses. We included studies reporting T1 mapping mainly in PAH and excluding other PH groups to limit disease heterogeneity. However, the included studies included 6% of patients with CTEPH and 1% of other types of PH which might have introduced some heterogeneity.

5. Conclusion

T_1 mapping values in PAH patients are on average 9% higher than healthy controls when assessed under the same conditions including the same MRI system, magnetic field strength or sequence used for acquisition. The highest T_1 and ECV values are at the RV insertion points. T_1 values and ECV in PH are higher than the values reported in cardiomyopathies and were associated with poor RV function and RV dilatation.

Ethics approval

Not applicable.

Consent for publication

Not applicable.

Availability of data and material

All data generated or analysed during this study are included in this published article [and its supplementary information files].

Funding

This work was supported by the Wellcome Trust awards (215799/Z/19/Z and 205188/Z/16/Z).

Authors' contributions

SA, DGK, JMW, AJS conceived the idea for the study.
SA screened the studies for inclusion.
SA, LS, AJS contributed to study design.
SA, AJS, YS contributed to the study analysis.
SA, PG, FAA contributed to data extraction, risk of bias analysis and.
SA, LS, PG drafted the manuscript.
AR, VOP, EN, DGK, AJS provided clinical expertise and general advice, and revised the manuscript.
All authors reviewed and approved the final manuscript.
All authors listed have contributed sufficiently to the project to be included as authors, and all those who are qualified to be authors are listed in the author byline. To the best of our knowledge, no conflict of interest, financial or other, exists.

Declaration of Competing Interest

None.

Acknowledgements

Not applicable.

Appendix A. Supplementary data

Supplementary data to this article can be found online at https://doi.org/10.1016/j.mri.2021.03.011.

References

[1] Haaf P, Garg P, Messroghli DR, et al. Cardiac T1 mapping and extracellular volume (ECV) in clinical practice: a comprehensive review. J Cardiovasc Magn Reson 2016;18:89.
[2] Puntmann VO, Peker E, Chandrashekhar Y, Nagel E. T1 mapping in characterizing myocardial disease: a comprehensive review. Circ Res 2016;119:277–99.
[3] Messroghli DR, Plein S, Higgins DM, et al. Human myocardium: single-breath-hold MR T1 mapping with high spatial resolution–reproducibility study. Radiology 2006;238:1004–12.
[4] Garg P, Saunders LC, Swift AJ, et al. Role of cardiac T1 mapping and extracellular volume in the assessment of myocardial infarction. Anatol J Cardiol 2018;19:404–11.
[5] Bull S, White SK, Piechnik SK, et al. Human non-contrast T1 values and correlation with histology in diffuse fibrosis. Heart 2013;99:932–7.
[6] Ferreira VM, Piechnik SK, Dall'Armellina E, et al. Non-contrast T1-mapping detects acute myocardial edema with high diagnostic accuracy: a comparison to T2-weighted cardiovascular magnetic resonance. J Cardiovasc Magn Reson 2012;14:42.
[7] Karamitsos TD, Piechnik SK, Banypersad SM, et al. Noncontrast T1 mapping for the diagnosis of cardiac amyloidosis. JACC Cardiovasc Imaging 2013;6:488–97.
[8] Ugander M, Bagi PS, Oki AJ, et al. Myocardial edema as detected by pre-contrast T1 and T2 CMR delineates area at risk associated with acute myocardial infarction. JACC Cardiovasc Imaging 2012;5:596–603.
[9] Dall'Armellina E, Piechnik SK, Ferreira VM, et al. Cardiovascular magnetic resonance by non contrast T1-mapping allows assessment of severity of injury in acute myocardial infarction. J Cardiovasc Magn Reson 2012;14:15.
[10] Dass S, Suttie JJ, Piechnik SK, et al. Myocardial tissue characterization using magnetic resonance noncontrast t1 mapping in hypertrophic and dilated cardiomyopathy. Circ Cardiovasc Imaging 2012;5:726–33.
[11] Kuruvilla S, Janardhanan R, Antkowiak P, et al. Increased extracellular volume and altered mechanics are associated with LVH in hypertensive heart disease, not hypertension alone. JACC Cardiovasc Imaging 2015;8:172–80.
[12] Mascherbauer J, Marzluf BA, Tufaro C, et al. Cardiac magnetic resonance postcontrast T1 time is associated with outcome in patients with heart failure and preserved ejection fraction. Circ Cardiovasc Imaging 2013;6:1056–65.
[13] Messroghli DR, Moon JC, Ferreira VM, et al. Clinical recommendations for cardiovascular magnetic resonance mapping of T1, T2, T2* and extracellular volume: a consensus statement by the Society for Cardiovascular Magnetic Resonance (SCMR) endorsed by the European Association for Cardiovascular Imaging (EACVI). J Cardiovasc Magn Reson 2017;19:75.
[14] Moon JC, Messroghli DR, Kellman P, et al. Myocardial T1 mapping and extracellular volume quantification: a Society for Cardiovascular Magnetic Resonance (SCMR) and CMR working Group of the European Society of cardiology consensus statement. J Cardiovasc Magn Reson 2013;15:92.
[15] Nakamori S, Dohi K, Ishida M, et al. Native T1 mapping and extracellular volume mapping for the assessment of diffuse myocardial fibrosis in dilated cardiomyopathy. JACC Cardiovasc Imaging 2018;11:48–59.
[16] Puntmann VO, Voigt T, Chen Z, et al. Native T1 mapping in differentiation of normal myocardium from diffuse disease in hypertrophic and dilated cardiomyopathy. JACC Cardiovasc Imaging 2013;6:475–84.
[17] Mikami Y, Alfagih R, Khan A, et al. Value of non-contrast T1 mapping MRI for the differentiation of hypertrophic cardiomyopathy, cardiac amyloid and FABRY cardiomyopathy. Can J Cardiol 2017;33:S22.
[18] Pagano JJ, Chow K, Khan A, et al. Reduced right ventricular native myocardial T1 in Anderson-Fabry disease: comparison to pulmonary hypertension and healthy controls. PLoS One 2016;11:e0157565.
[19] Sado DM, White SK, Piechnik SK, et al. Identification and assessment of Anderson-Fabry disease by cardiovascular magnetic resonance noncontrast myocardial T1 mapping. Circ Cardiovasc Imaging 2013;6:392–8.
[20] Thompson Richard B, Kelvin Chow, Aneal Khan, et al. T1 mapping with cardiovascular MRI is highly sensitive for Fabry disease independent of hypertrophy and sex. Circ Cardiovasc Imaging 2013;6:637–45.
[21] Wilson HC, Ambach S, Madueme PC, et al. Comparison of native T1, strain, and traditional measures of cardiovascular structure and function by cardiac magnetic resonance imaging in patients with Anderson-Fabry disease. Am J Cardiol 2018;122:1074–8.
[22] Krittayaphong R, Zhang S, Saiviroonporn P, et al. Assessment of cardiac Iron overload in thalassemia with MRI on 3.0-T: high-field T1, T2, and T2* quantitative parametric mapping in comparison to T2* on 1.5-T. JACC Cardiovasc Imaging 2019;12:752–4.
[23] Torlasco C, Cassinerio E, Roghi A, et al. Role of T1 mapping as a complementary tool to T2* for non-invasive cardiac iron overload assessment. PLoS One 2018;13:e0192890.
[24] Cui Y, Cao Y, Song J, et al. Association between myocardial extracellular volume and strain analysis through cardiovascular magnetic resonance with histological myocardial fibrosis in patients awaiting heart transplantation. J Cardiovasc Magn Reson 2018;20:25.
[25] Kammerlander A, Tufaro C, Bachmann AF, et al. Extracellular matrix expansion by cardiac magnetic resonance T1 mapping- validation with myocardial biopsy. J Cardiovasc Magn Reson 2015;17:P308.

[26] Wong TC, Piehler K, Meier CG, et al. Association between extracellular matrix expansion quantified by cardiovascular magnetic resonance and short-term mortality. Circulation 2012;126:1206–16.
[27] Puntmann VO, Carr-White G, Jabbour A, et al. Native T1 and ECV of noninfarcted myocardium and outcome in patients with coronary artery disease. J Am Coll Cardiol 2018;71:766–78.
[28] Puntmann VO, Carr-White G, Jabbour A, et al. T1-mapping and outcome in nonischemic cardiomyopathy: all-cause mortality and heart failure. JACC Cardiovasc Imaging 2016;9:40–50.
[29] Andersen S, Nielsen-Kudsk JE, Vonk Noordegraaf A, de Man FS. Right ventricular fibrosis. Circulation 2019;139:269–85.
[30] Kiely DG, Levin D, Hassoun P, et al. EXPRESS: statement on imaging and pulmonary hypertension from the pulmonary vascular research institute (PVRI). Pulm Circ 2019;9(3). 2045894019841990.
[31] Gottbrecht M, Kramer CM, Salerno M. Native T1 and extracellular volume measurements by cardiac MRI in healthy adults: a meta-analysis. Radiology 2019; 290:317–26.
[32] Zhuang B, Sirajuddin A, Wang S, et al. Prognostic value of T1 mapping and extracellular volume fraction in cardiovascular disease: a systematic review and meta-analysis. Heart Fail Rev 2018;23:723–31.
[33] Minegishi S, Kato S, Takase-Minegishi K, et al. Native T1 time and extracellular volume fraction in differentiation of normal myocardium from non-ischemic dilated and hypertrophic cardiomyopathy myocardium: a systematic review and meta-analysis. Int J Cardiol Heart Vasc 2019;25:100422.
[34] van den Boomen M, Riemer HJ, Hulleman EV, et al. Native T 1 reference values for nonischemic cardiomyopathies and populations with increased cardiovascular risk: a systematic review and meta-analysis. J Magn Reson Imaging 2018;47:891–912.
[35] Sterne JAC, Egger M, Moher D. Addressing reporting biases. In: Cochrane handbook for systematic reviews of interventions; 2021. p. 297–333.
[36] Chen YY, Yun H, Jin H, et al. Association of native T1 times with biventricular function and hemodynamics in precapillary pulmonary hypertension. Int J Cardiovasc Imaging 2017;33:1179–89.
[37] Homsi R, Luetkens JA, Skowasch D, et al. Left ventricular myocardial fibrosis, atrophy, and impaired contractility in patients with pulmonary arterial hypertension and a preserved left ventricular function: a cardiac magnetic resonance study. J Thorac Imaging 2017;32:36–42.
[38] Mehta BB, Auger DA, Gonzalez JA, et al. Detection of elevated right ventricular extracellular volume in pulmonary hypertension using accelerated and navigator-gated look-locker imaging for cardiac T1 estimation (ANGIE) cardiovascular magnetic resonance. J Cardiovasc Magn Reson 2015;17:110.
[39] Patel RB, Li E, Benefield BC, et al. Diffuse right ventricular fibrosis in heart failure with preserved ejection fraction and pulmonary hypertension. ESC Heart Fail 2020; 7:253–63.
[40] Reiter U, Reiter G, Kovacs G, et al. Native myocardial T1 mapping in pulmonary hypertension: correlations with cardiac function and hemodynamics. Eur Radiol 2017;27:157–66.
[41] Saunders LC, Johns CS, Stewart NJ, et al. Diagnostic and prognostic significance of cardiovascular magnetic resonance native myocardial T1 mapping in patients with pulmonary hypertension. J Cardiovasc Magn Reson 2018;20:78.
[42] Spruijt OA, Vissers L, Bogaard H-J, et al. Increased native T1-values at the interventricular insertion regions in precapillary pulmonary hypertension. Int J Cardiovasc Imaging 2016;32:451–9.
[43] Tello K, Dalmer A, Axmann J, et al. Reserve of right ventricular-arterial coupling in the setting of chronic overload. Circ Heart Fail 2019;12:e005512.
[44] Wang J, Zhao H, Wang Y, et al. Native T1 and T2 mapping by cardiovascular magnetic resonance imaging in pressure overloaded left and right heart diseases. J Thorac Dis 2018;10:2968–75.
[45] Ryotaro Asano, Takeshi Ogo, Yoshiaki Morita, et al. Abstract 15190: native T1 mapping: a novel prognostic marker in pulmonary hypertension. Circulation 2018; 138. A15190–A15190.
[46] Habert P, Capron T, Hubert S, et al. Quantification of right ventricular extracellular volume in pulmonary hypertension using cardiac magnetic resonance imaging. Diagn Interv Imaging 2020;101:311–20.
[47] Dong Y, Sun J, Yang D, et al. Right ventricular septomarginal trabeculation hypertrophy is associated with disease severity in patients with pulmonary arterial hypertension. Int J Cardiovasc Imaging 2018;34:1439–49.
[48] Swift AJ, Rajaram S, Capener D, et al. LGE patterns in pulmonary hypertension do not impact overall mortality. JACC Cardiovasc Imaging 2014;7:1209–17.
[49] Broberg CS, Prasad SK, Carr C, et al. Myocardial fibrosis in Eisenmenger syndrome: a descriptive cohort study exploring associations of late gadolinium enhancement with clinical status and survival. J Cardiovasc Magn Reson 2014;16.
[50] Blyth KG, Groenning BA, Martin TN, et al. Contrast enhanced-cardiovascular magnetic resonance imaging in patients with pulmonary hypertension. Eur Heart J 2005;26:1993–9.
[51] Bratis K, Lindholm A, Hesselstrand R, et al. CMR feature tracking in cardiac asymptomatic systemic sclerosis: clinical implications. PLoS One 2019;14: e0221021.
[52] Ntusi NAB, Piechnik SK, Francis JM, et al. Subclinical myocardial inflammation and diffuse fibrosis are common in systemic sclerosis – a clinical study using myocardial T1-mapping and extracellular volume quantification. J Cardiovasc Magn Reson 2014;16:21.
[53] Brown J, Norrington K, Kotecha T, et al. P5262Subclinical myocardial abnormalities in systemic sclerosis-associated versus non-connective tissue disease pulmonary hypertension by CMR multiparametric mapping. Eur Heart J 2019;40.
[54] Jellis CL, Yingchoncharoen T, Gai N, et al. Correlation between right ventricular T1 mapping and right ventricular dysfunction in non-ischemic cardiomyopathy. Int J Cardiovasc Imaging 2018;34:55–65.
[55] Swift AJ, Capener D, Johns C, et al. Magnetic resonance imaging in the prognostic evaluation of patients with pulmonary arterial hypertension. Am J Respir Crit Care Med 2017;196:228–39.
[56] Alabed S, Shahin Y, Garg P, et al. Cardiac MRI and prediction of clinical worsening and mortality in pulmonary arterial hypertension: a systematic review and meta-analysis. J Am Coll Cardiol Img 2020. https://doi.org/10.1016/j.jcmg.2020.08.013.
[57] McCann GP, Beek AM, Vonk-Noordegraaf A, van Rossum AC. Delayed contrast-enhanced magnetic resonance imaging in pulmonary arterial hypertension. Circulation 2005;112:e268.
[58] Sanz J, Dellegrottaglie S, Kariisa M, et al. Prevalence and correlates of septal delayed contrast enhancement in patients with pulmonary hypertension. Am J Cardiol 2007;100:731–5.
[59] Freed BH, Gomberg-Maitland M, Chandra S, et al. Late gadolinium enhancement cardiovascular magnetic resonance predicts clinical worsening in patients with pulmonary hypertension. J Cardiovasc Magn Reson 2012;14:11.
[60] De Lazzari M, Cipriani A, Rizzo S, et al. Right ventricular junctional late gadolinium enhancement correlates with outcomes in pulmonary hypertension. JACC Cardiovasc Imaging 2019;12:936–8.
[61] Roller FC, Wiedenroth C, Breithecker A, et al. Native T1 mapping and extracellular volume fraction measurement for assessment of right ventricular insertion point and septal fibrosis in chronic thromboembolic pulmonary hypertension. Eur Radiol 2017;27:1980–91.
[62] García-Álvarez A, García-Lunar I, Pereda D, et al. Association of myocardial T1-mapping CMR with hemodynamics and RV performance in pulmonary hypertension. JACC Cardiovasc Imaging 2015;8:76–82.
[63] Kellman P, Hansen MS. T1-mapping in the heart: accuracy and precision. J Cardiovasc Magn Reson 2014;16:2.
[64] Jang J, Ngo LH, Captur G, et al. Measurement reproducibility of slice-interleaved T1 and T2 mapping sequences over 20 months: a single center study. PLoS One 2019;14:e0220190.
[65] Rogers T, Dabir D, Mahmoud I, et al. Standardization of T1 measurements with MOLLI in differentiation between health and disease–the ConSept study. J Cardiovasc Magn Reson 2013;15:78.
[66] Zhu Y, Fahmy AS, Duan C, et al. Automated myocardial T2 and extracellular volume quantification in cardiac MRI using transfer learning-based myocardium segmentation. Radiol Artif Intell 2020;2:e190034.
[67] Raman FS, Kawel-Boehm N, Gai N, et al. Modified look-locker inversion recovery T1 mapping indices: assessment of accuracy and reproducibility between magnetic resonance scanners. J Cardiovasc Magn Reson 2013;15:64.
[68] Fortin J-P, Sweeney EM, Muschelli J, et al. Removing inter-subject technical variability in magnetic resonance imaging studies. Neuroimage 2016;132: 198–212.
[69] Fortin J-P, Parker D, Tunç B, et al. Harmonization of multi-site diffusion tensor imaging data. Neuroimage 2017;161:149–70.